



Contents lists available at ScienceDirect

## Clinical Nutrition

journal homepage: <http://www.elsevier.com/locate/clnu>

## Original article

# Gut microbiota alterations induced by intensive chemotherapy in acute myeloid leukaemia patients are associated with gut barrier dysfunction and body weight loss



Sarah A. Pötgens<sup>a,1</sup>, Sophie Lecop<sup>a,1</sup>, Violaine Havelange<sup>b,c</sup>, Fuyong Li<sup>d,e</sup>,  
Audrey M. Neyrinck<sup>a</sup>, Nathalie Neveux<sup>f</sup>, Johan Maertens<sup>g,h</sup>, Jens Walter<sup>i</sup>,  
Hélène Schoemans<sup>j,k</sup>, Nathalie M. Delzenne<sup>a</sup>, Laure B. Bindels<sup>a,l,\*</sup>

<sup>a</sup> Metabolism and Nutrition Research Group, Louvain Drug Research Institute, UCLouvain, Université catholique de Louvain, Brussels, Belgium

<sup>b</sup> Department of Hematology, Cliniques Universitaires Saint-Luc, UCLouvain, Université catholique de Louvain, Brussels, Belgium

<sup>c</sup> Experimental Medicine Unit, De Duve Institute, UCLouvain, Université catholique de Louvain, Brussels, Belgium

<sup>d</sup> Department of Infectious Diseases and Public Health, Jockey Club College of Veterinary Medicine and Life Sciences, City University of Hong Kong, Kowloon, Hong Kong SAR, China

<sup>e</sup> Department of Agricultural, Food and Nutritional Science, University of Alberta, Edmonton, Alberta, Canada

<sup>f</sup> Clinical Chemistry Department, Cochin Hospital, Paris Centre University Hospitals, Paris, France

<sup>g</sup> Department of Hematology, University Hospital Gasthuisberg, Leuven, Belgium

<sup>h</sup> Department of Microbiology, Immunology and Transplantation, KU Leuven, Leuven, Belgium

<sup>i</sup> Department of Medicine, School of Microbiology, APC Microbiome Ireland, University College Cork, Cork, Ireland

<sup>j</sup> Department of Hematology, University Hospitals Leuven, Leuven, Belgium

<sup>k</sup> Department of Public Health and Primary Care, ACCENT VV, KU Leuven - University of Leuven, Leuven, Belgium

<sup>l</sup> Welbio Department, WEL Research Institute, Wavre, Belgium

## ARTICLE INFO

## Article history:

Received 11 June 2023

Accepted 21 September 2023

## Keywords:

Cachexia

Microbiome

Antibiotics

Chemotherapy

Anorexia

Gut permeability

## SUMMARY

**Background & aims:** Acute myeloid leukaemia (AML) chemotherapy has been reported to impact gut microbiota composition. In this study, we investigated using a multi-omics strategy the changes in the gut microbiome induced by AML intense therapy and their association with gut barrier function and cachectic hallmarks.

**Methods:** 10 AML patients, allocated to standard induction chemotherapy (SIC), were recruited. Samples and data were collected before any therapeutic intervention (T0), at the end of the SIC (T1) and at discharge (T4). Gut microbiota composition and function, markers of inflammation, metabolism, gut barrier function and cachexia, as well as faecal, blood and urine metabolomes were assessed.

**Results:** AML patients demonstrated decreased appetite, weight loss and muscle wasting during hospitalization, with an incidence of cachexia of 50%. AML intensive treatment transiently impaired the gut barrier function and led to a long-lasting change of gut microbiota composition characterized by an important loss of diversity. *Lactobacillaceae* and *Campylobacter concisus* were increased at T1 while *Enterococcus faecium* and *Staphylococcus* were increased at T4. Metabolomics analyses revealed a reduction in urinary hippurate and faecal bacterial amino acid metabolites (bAAM) (2-methylbutyrate, isovalerate, phenylacetate). Integration using DIABLO revealed a deep interconnection between all the datasets. Importantly, we identified bacteria which disappearance was associated with impaired gut barrier function (*Odoribacter splanchnicus*) and body weight loss (*Gemmiger formicilis*), suggesting these bacteria as actionable targets.

**Conclusion:** AML intensive therapy transiently impairs the gut barrier function while inducing enduring alterations in the composition and metabolic activity of the gut microbiota that associate with body weight loss.

**Trial registration:** NCT03881826, <https://clinicaltrials.gov/ct2/show/NCT03881826>.

© 2023 The Authors. Published by Elsevier Ltd. This is an open access article under the CC BY-NC-ND license (<http://creativecommons.org/licenses/by-nc-nd/4.0/>).

\* Corresponding author. Metabolism and Nutrition Research Group, Louvain Drug Research Institute, UCLouvain, Université catholique de Louvain, avenue E. Mounier box B1.73.11, B-1200 Brussels, Belgium.

E-mail address: [laure.bindels@uclouvain.be](mailto:laure.bindels@uclouvain.be) (L.B. Bindels).

<sup>1</sup> Equally contributed to this work.

## 1. Introduction

Acute myeloid leukaemia (AML) is a clonal disorder of the hematopoietic stem cells resulting in impaired production of the myeloid blood cell lineage [1]. Standard treatment for fit AML patients (<65 years) is intensive induction chemotherapy followed by a consolidation chemotherapy and an allogeneic hematopoietic stem cell transplantation (HSCT) following the risk of relapse. The standard induction chemotherapy (SIC) is a combination of 7 days of cytarabine and 3 days of anthracycline such as idarubicin or daunorubicin (7 + 3 regimen), with a 70–80% initial complete remission rate [2,3]. This treatment induces a prolonged aplasia associated with infections, leading to multiple and extended exposure to antibiotics. Altogether, patients undergoing AML intensive treatment are exposed to a combination of chemotherapeutic and antibiotic drugs. The impact of such intensive treatment on the microbiota and its ensuing consequences has raised interest. Several studies looked at the gut microbiota alterations caused by SIC [4–6] while others focused on the role of the impaired gut microbiota in neutropenic fever [7–9] and graft-versus-host disease development [10–12].

The combination of cytotoxic and antibiotic therapy also deeply impacts intestinal homeostasis. Indeed, cytotoxic therapies (including those used in AML) have been shown to impair gut barrier integrity [13,14]. In addition, antibiotics disrupt the gut microbiota, resulting in a loss of microbial diversity [6,15]. This will in turn impair the microbiome-mediated colonization resistance and lead to an overgrowth of pathobionts enriched in antibiotic resistance genes [16]. Bacterial translocation is facilitated, and the risk of bloodstream infection increases [17]. Another consequence of such therapy is the persistent reduction in some beneficial bacterial species, like *Faecalibacterium prausnitzii* and *Bifidobacterium* spp., even after the completion of chemotherapy [4]. Recent data have shown the long-lasting effect of AML treatments suggesting that the gut microbiota of AML patients is still altered 6 months after therapy [18].

The impact of intensive AML therapy is not limited to the gut microbiota and the intestinal homeostasis. SIC may alter body composition, and particularly the muscle compartment. Body weight, and skeletal muscle mass in particular, emerges as an important prognostic factor for survival [19–21]. Weight loss is a central aspect of cachexia pathophysiology which is related to an increase in pro-inflammatory cytokines. In cancer patients with cachexia, (interleukin 6) IL6, (tumor necrosis factor- $\alpha$ ) TNF- $\alpha$  and to a lesser extent (interleukin 8) IL8 are increased compared to in healthy individuals but only IL6 is increased compared to cancer patients without cachexia [22]. Although cachexia affects 40% of the patients with hematological cancer [23] and is often witnessed in clinics, studies focusing on AML therapy-related cachexia are scarce [24]. Since we have previously demonstrated that counteracting gut microbiota alterations using rationally selected pre- and probiotics was able to improve cachectic features in leukemic mice [25–27], we aimed to explore the associations between gut microbiome alterations and cachectic features in AML patients using a multi-omics approach.

Multi-omics analyses can assess different but related aspects of pathogenesis which are often causally linked [28]. Importantly, knowledge obtained from longitudinal multi-omics studies facilitate the generation of testable hypotheses for subsequent pre-clinical investigation and therapeutic trials [28,29]. Therefore, to get a deeper knowledge on the impact of the AML intensive treatment on the gut microbiota of AML patients and their links to cachectic hallmarks and gut barrier function, we applied such multi-omics integrative approach on a deeply characterised exploratory cohort.

## 2. Methods

### 2.1. Subjects

10 patients newly diagnosed with AML were recruited between December 2015 and December 2019 among two Belgian University hospitals (Saint-Luc Brussels (n = 3), UZ Leuven (n = 7)). The inclusion criteria were as follows: (i) a diagnosis of AML and related precursor neoplasms according to WHO 2008 classification (excluding acute promyelocytic leukaemia) including secondary AML (after an antecedent haematological disease (e.g. MDS) and therapy-related AML) OR acute leukaemia's of ambiguous lineage according to WHO 2008 OR a diagnosis of refractory anaemia with excess of blasts (MDS REAB) 2 and IPSS (International Prognostic Scoring System)-R score > 2; (ii) treatment combining aracytine (cytarabine 200 mg/m<sup>2</sup> for 7 days) and an anthracycline (idarubicin 12 mg/m<sup>2</sup> or daunorubicin 45 mg/m<sup>2</sup> for 3 days) according to the conventional 7 + 3 regimen; (iii) World Health Organization performance status 0, 1 or 2; (iv) sampled bone marrow and/blood cells at diagnosis with molecular analysis; (v) written informed consent; (v) good command of the French or Dutch language. Exclusion criteria were as follows: age below 18 or above 75 years, pregnancy, antibiotics consumption within the last 30 days, recent chemotherapy (<3 months), with exclusion of hydroxyurea, obesity (BMI > 30), any history of chronic intestinal affections (Crohn disease, inflammatory bowel disease, gluten intolerance), gastric bypass, ongoing treatment with antidiabetic or hypoglycaemic drugs. This study was approved by the "Comité d'éthique Hospitalo-facultaire des Cliniques Universitaires Saint-Luc" (B403201317128, NCT03881826) and all participants provided written informed consent. A full description of the study design is provided in the Supporting Information.

### 2.2. Sample and data collection

All biological sampling and data collection were performed at the time of diagnosis, before the beginning of the chemotherapy treatment and the administration of any antibiotics (T0), the first working day after the end of chemotherapy (T1) and the day of discharge (i.e. T4, on average 4 weeks after T0) (Fig. 1A, Fig. S1).

Case report forms were collected with medical history, oral and gastrointestinal adverse events, drug records including consumption of prebiotics, probiotics and antibiotics, as well as lab assessment of haemoglobin, WBCC, C-reactive protein (CRP), albumin and glycaemia levels. Body composition and muscle strength were assessed by bioimpedancemetry and a Jamar hand dynamometer, respectively. Appetite was evaluated using the simplified nutritional assessment questionnaire (SNAQ) [30]. Full details on the questionnaire and sample management are provided in the Supporting Information.

### 2.3. Biochemical analyses

Citrulline was measured in plasma (EDTA) using ion exchange chromatography as described in Neveux et al. [31]. Plasma cytokines and hormones were measured using a customized U-plex kit and a Meso Scale Discovery microplate reader (Meso Scale Discovery, USA). LBP levels were assessed using an ELISA kit (Hycult-Biotech, PA, USA). Full list and details on these procedures are provided in the Supporting Information.

### 2.4. Gut microbiome analyses

DNA was extracted from stools following the protocol Q [32]. This protocol uses the QIAamp DNA Stool Mini Kit (Qiagen,

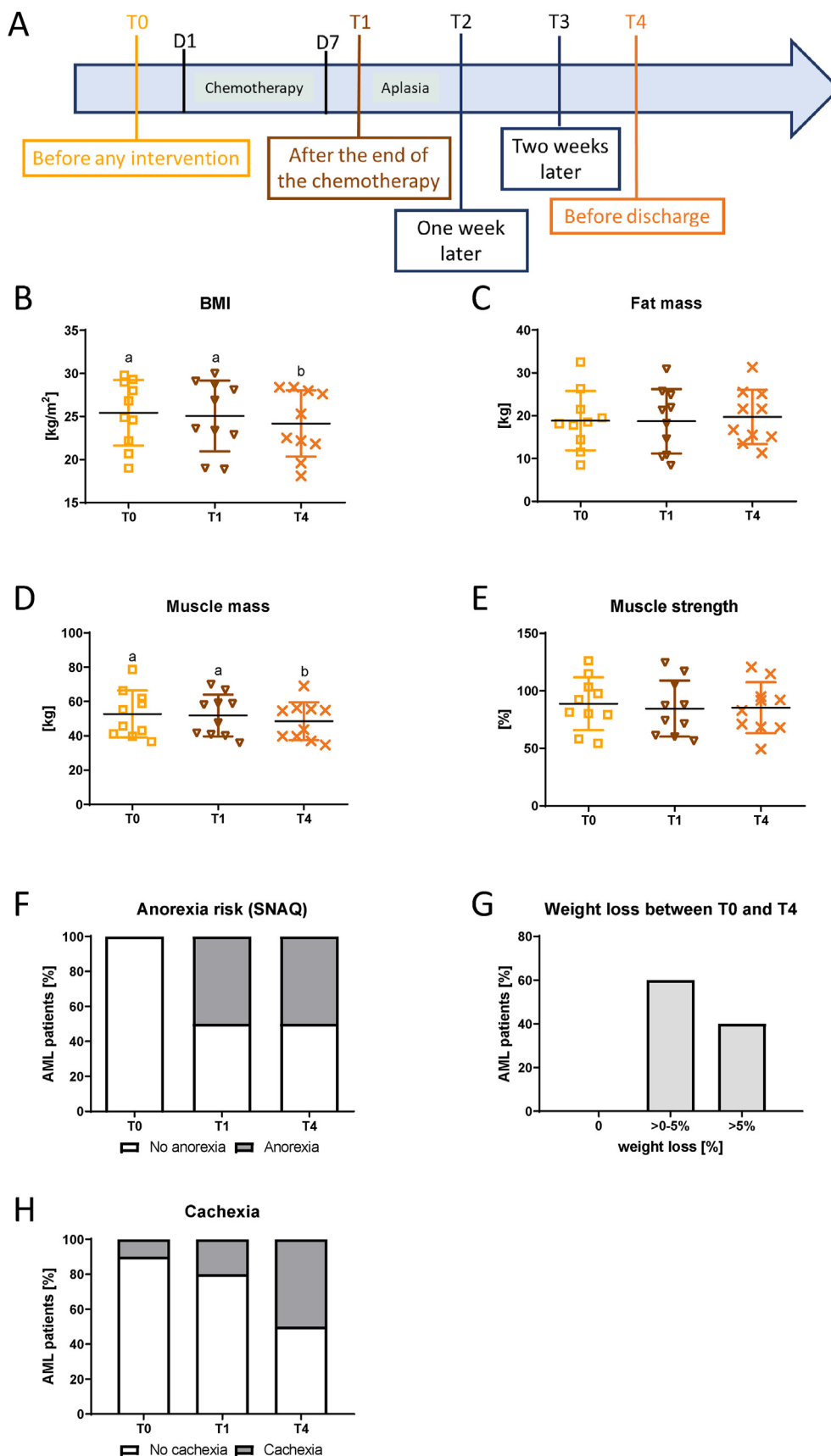


**Fig. 1.** Bodyweight, muscle strength and appetite evolution through chemotherapy. A) Timeline presentation of the experimental design. B) Body mass index (BMI). C) Fat mass. D) Muscle mass. E) Muscle strength. F) Results of the SNAQ score in %. Anorexia is attributed to scores  $\leq 14$ . Fisher's test: p-value  $< 0.05$ . G) Percentage of weight loss between diagnosis and discharge. H) Cachectic patients in % according to Fearon's definition. B-E are normally distributed data and expressed as mean (standard deviation) and tested with a fixed-effect analysis (Tukey's post-tests). Groups with different superscript letters are significantly different.

Germany) and includes a bead-beating step. The DNA was analysed using 16S rRNA gene sequencing and shotgun sequencing. Sequencing procedures, as well as bioinformatics and biostatistics analyses are detailed in the Supporting Information. Raw sequences can be found in the SRA database (projects ID: PRJNA813705 (T0) and PRJNA875377 (T1-T4)).

### 2.5. <sup>1</sup>H-NMR metabolomics analyses

Faecal, blood and urine samples were prepared in adequate phosphate buffer (pH = 7) with trimethylsilylpropanoic acid (TSP) as standard. NMR was performed on a Bruker Avance 600 MHz NMR spectrometer equipped with a cryoprobe. They were further processed using MestReNova (v14.2) and analysed as previously described [33]. Metabolites were assigned using the Chenomx NMR Suite (v8.43), the Bruker B-BIORECODE database (Amix software v3.9.15), the HMDB [34] and additional 2D NMR experiments on selected representative samples. The Chenomx NMR Suite was used to perform a relative quantification of the concentration of identified metabolites. Full details on these procedures are provided in the Supporting Information.

### 2.6. Statistical analyses

For continuous variables, normality was assessed using d'Agostino and Pearson omnibus normality test. If normality was not respected in one group, the non-parametric Friedman test was used. When p-value < 0.05, Dunn's post-tests were performed. If normality was respected, a mixed-effects analysis was performed. When p-value < 0.05, Tukey's post-tests were performed. Coherently, normal variables are presented as mean with standard deviation (SD) whereas non-normal variables are presented as median with interquartile range (IQR). For categorical variables, a Fisher test was performed. For all -omics data, normality was not assessed, and Friedman tests were therefore used with Dunn's post-tests when appropriate. When needed, a correction for FDR was applied [35]. To determine the different profiles in the changes observed for all metabolites over time, we used the *Mfuzz* R package implementing C-means clustering [36]. To integrate the different data collected, we used DIABLO: Data Integration Analysis for Biomarker discovery using Latent cOmponents [37], part of the *mixOmics* R package [38]. Spearman correlations were performed to answer specific questions such as the correlation between the level of *Odoribacter splanchnicus* and the change in LBP and citrulline levels between T1 and T0. P < 0.05 was considered statistically significant. Statistical analyses were performed using GraphPad Prism 8.0.1 and R. Full details concerning statistical analyses are provided in the Supporting Information.

## 3. Results

Ten patients consecutively diagnosed with AML and meeting the inclusion criteria were prospectively recruited. At three time points, namely before any therapeutic intervention, at the end of the SIC and before discharge, we collected biological samples and clinical data (Fig. 1A, Fig. S1). General characteristics of the patients are presented in Table 1, with a description of their medication in Table S1. Body mass index (BMI) and muscle mass were significantly decreased at T4 whereas fat mass and muscle strength were not altered (Fig. 1B-E). After chemotherapy (T1 and T4), half of the patients were at risk for anorexia according to the SNAQ questionnaire and all of them had lost weight at the time of discharge (Fig. 1F-G). According to Fearon's definition [39], half of the patients were cachectic at discharge (T4) (Fig. 1H).

**Table 1**

Baseline characteristics of study participants and antimicrobial drugs administered during the hospitalization.<sup>a</sup>

| characteristics   | Patients    |
|---|-------------|
| Age, y  | 53.6 (13.8) |
| Sex, %  |             |
| Female  | 50          |
| Male  | 50          |
| Bmi, kg/m <sup>2</sup>  | 25.4 (3.8)  |
| Lean mass, %  | 70.4 (9.3)  |
| Fat mass, %   | 25.9 (9.8)  |
| Smoker, %   | 20          |
| Antibiotics during induction phase (T0-T1), %                                   | 90          |
| Meropenem   | 30          |
| Piperacillin + tazobactam   | 10          |
| Levofloxacin  | 60          |
| Antifungal medications during induction phase (T0-T1), %                        | 100         |
| Fluconazole   | 90          |
| Posaconazole  | 10          |
| Miconazole  | 10          |
| Caspofungin   | 10          |
| Antiviral medications during induction phase (T0-T1), %                         | 20          |
| Acyclovir   | 20          |
| Antibiotics between the end of chemotherapy and discharge (T1-T4), %            | 100         |
| Meropenem   | 80          |
| Piperacillin + tazobactam   | 10          |
| Levofloxacin  | 50          |
| Cerufloxime   | 10          |
| Vancomycin  | 20          |
| Antifungal medications between the end of chemotherapy and discharge (T1-T4), % | 90          |
| Fluconazole   | 80          |
| Caspofungin   | 20          |
| Antiviral medications between the end of chemotherapy and discharge (T1-T4), %  | 20          |
| Acyclovir   | 20          |

<sup>a</sup> Variables that are normally distributed are expressed as mean (standard deviation). Frequency distributions are expressed as percentage.

Various metabolic and inflammatory markers were measured (Table S2). After chemotherapy, AML patients displayed a decrease in haemoglobin and white blood cell count (WBCC), characteristic of the treatment. Levels of C-reactive protein (CRP), IL6, IL8 and monocyte chemoattractant protein 1 (MCP1) reflected a higher inflammatory status at T1 which was reduced at discharge. To better understand the biological drivers of anorexia, two key appetite regulators, ghrelin and the growth differentiation factor 15 (GDF15), were measured in the serum of the patients (Fig. 2A). The increase at T1 was significant for GDF15. GDF15 has been shown to mediate platinum-based chemotherapy-induced anorexia and body weight loss in mice and nonhuman primates [40] and its production is induced in mononuclear cells exposed to cytarabine [41], raising the likelihood that GDF15 may also contribute to IC-induced anorexia. The fibroblast growth factor 21 (FGF21) is an emerging target in cancer cachexia as this hormone can induce muscle loss [42] and was therefore also measured. FGF21 was reduced by 5-fold at T1 (Table S2), excluding the implication of FGF21 in the treatment-induced muscle loss. In addition, plasma levels of citrulline, a non-proteinogenic amino acid (AA) reflecting functional enterocyte mass [43], was significantly decreased at T1 and restored at T4, while the level of the lipopolysaccharide-binding protein (LBP) showed an inverse profile (Fig. 2B, Fig. S2).

### 3.1. Impact of AML intensive treatment on gut microbiota composition

Patients received several drugs during their hospital stay, including anti-microbial drugs to prevent and/or treat infections, as

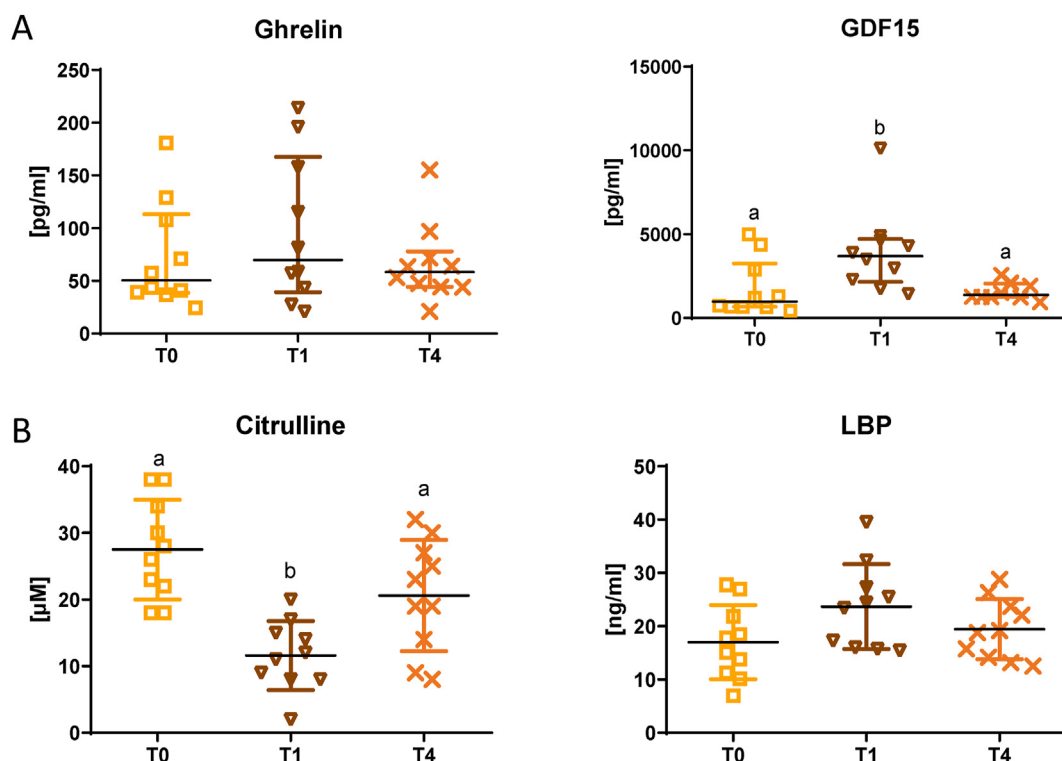


**Fig. 2.** Evolution of metabolic markers through chemotherapy. A) Markers linked to appetite regulation: ghrelin and growth differentiation factor 15 (GDF15). B) Markers linked to gut barrier: citrulline and lipopolysaccharide binding protein (LBP). Citrulline results presented here were obtained using a targeted MS-based assay. A are non-normally distributed data and expressed as median (interquartile range) and tested with a Friedman test (Dunn's post-tests). B are normally distributed data and expressed as mean (standard deviation) and tested with a fixed-effect analysis (Tukey's post-tests). LBP is statistically significantly affected after a fixed-effect analysis but no differences between timepoints were detected by the Tukey's post-tests. Groups with different superscript letters are significantly different.

appropriate (Table S3). 9 patients were administered antibiotics and all of them received antifungal medications during the week of the SIC. However, the nature of the antibiotics and antifungal medications were variable from one patient to another (Table 1). Despite the prolonged use of antibiotics in 9 patients out of 10, faecal bacterial load was not significantly affected at T1 and T4 (Fig. 3A). Six  $\alpha$ -diversity indexes were evaluated and showed the same trend towards reduction at T1 and T4. Significance was reached for Shannon and Simpson indexes, which combine the aspects of evenness and richness, as well as for Heip evenness and the indexes reflecting richness, namely Chao1 and observed ASV. Significance was not met by Simpson evenness index (Fig. 3B). Changes in the gut microbiota composition were also visible both at the genus and family levels (Figs. 4 and 5, Table S4). The gut microbiota composition was shifted at T1 without a return to the baseline situation at T4. Timing accounted respectively for 19.5% and 17.8% of the variance in the dataset at the genus and family levels. 17 families, 25 genera and 33 species were dramatically changed in their relative abundance ( $q$ -value < 0.05) over the timeframe of the hospitalization (Table S4). Among the 85 affected taxa, 41 were not detected at T1 and 62 at T4. The only taxa that were increased at T1 were the *Lactobacillaceae* family and *Campylobacter concisus* while taxa such as *Enterococcus faecium* (and parent genus and family) and *Staphylococcus* (and parent family) were detected only at T4. As metagenomics also allows the identification and quantification of bacterial enzymatic functions encoded in the faecal bacterial DNA, we also analysed those functions and found that 129 enzymatic functions were significantly altered ( $q$ -value < 0.1) (Table S5) while no metagenomics pathways (regrouping these functions) were found to be significantly affected after correction for multiple testing.

Besides those changes in the composition and functional potential of the gut microbiota, we also evaluated gastrointestinal adverse events and found that the occurrence of diarrhoea was higher at T1 compared to T0 and T4 (Fig. S3A, Table S2). Coherently, faecal samples at T1 exhibited a higher water content (Fig. S3B).

### 3.2. Impact of AML intensive treatment on faecal, blood and urine metabolites

Untargeted  $^1\text{H-NMR}$  metabolomics was used to analyse faecal, blood and urine samples at all timepoints (T0, T1 and T4).

PCA on faecal metabolites reflected the heterogeneity and diversity of response at T1 and a partial return to baseline at T4 (Fig. 6A). PERMANOVA revealed that 16.4% of the variance in the dataset is explained by the timing ( $p$ -value = 0.01). Using C-means clustering to regroup the metabolites by profiles, we found 5 clusters (Fig. 6B-C). All clusters except cluster 1 contained significantly altered metabolites (Fig. 6C, Fig. S4, Table S6A). Clusters 2, 4 and 5 regrouped metabolites that tended to be much higher at T1 than T0 and T4. Among the significantly altered metabolites of these clusters, the majority were AA. Cluster 3 grouped metabolites that tended to decrease at T1 and stay low at T4 in comparison to T0. Within this cluster, 2-methylbutyrate, isovalerate and phenylacetate, which are bacterial amino acid metabolites (bAAm) [44], were decreased at T1 and T4.

Serum metabolomics also revealed major changes and a higher heterogeneity in individual response to chemotherapy at T1 in comparison to baseline. However, the PCA (Fig. 7A) shows that ~3 weeks after the end of chemotherapy (T4), the serum metabolome came back closer to baseline than what was observed for the faecal metabolome (Fig. 6A). Timing explained 10.5% of the variance in the

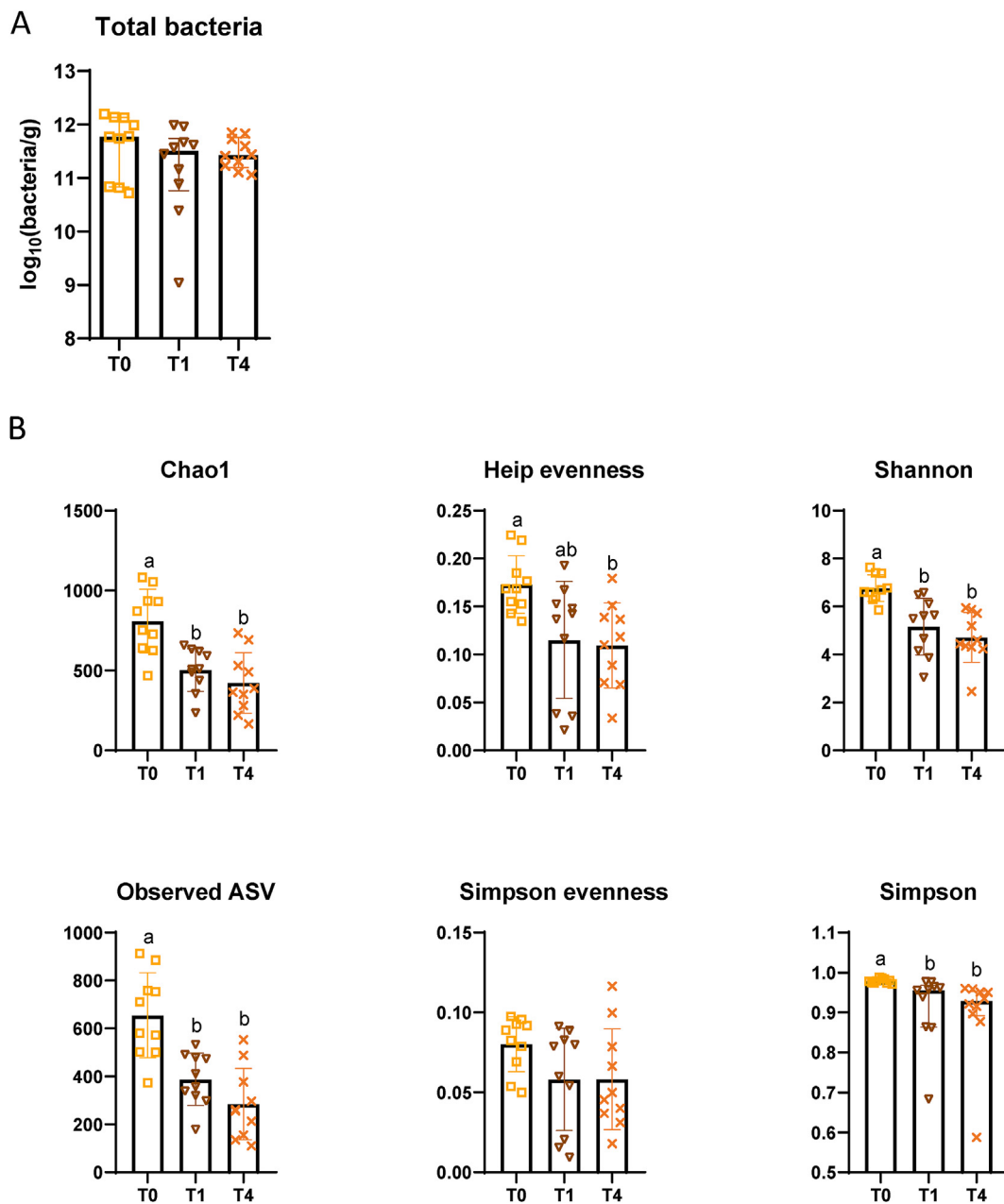


**Fig. 3.** Total bacteria and  $\alpha$ -diversity indexes through time. A) Total bacteria levels measured by qPCR. B)  $\alpha$ -diversity indexes. Chao1 and observed ASV are indexes of richness, Heip evenness and Simpson evenness are indexes of evenness while Shannon and Simpson are indexes combining the aspects of evenness and richness. Indexes that are normally distributed are expressed as mean (standard deviation) and are tested using a mixed-effect analysis (Tukey's post-tests). Total bacteria and indexes that are non-normally distributed are expressed as median (interquartile range) and are tested by a Friedman test (Dunn's post-tests). Groups with different superscript letters are significantly different.

dataset (PERMANOVA,  $p$ -value = 0.02). When using C-means clustering to cluster the metabolites by similar profiles, we found 3 clusters (Fig. 7B-C). All clusters contained significantly altered metabolites (Fig. 7C, Fig. S5, Table S6B). Metabolites in cluster 1 tended to decrease progressively through time such as the significantly reduced metabolites ornithine, myo-inositol, formate and dimethyl sulfone, members of this group. Cluster 2 contained metabolites which were mainly decreased at T1 and came back to similar levels as baseline at T4 such as proline, citrulline, succinate and dimethylamine. Among the significantly altered metabolites of cluster 3, 4 AA (valine, leucine, tyrosine and tryptophan) were increased at T1 and reduced at T4.

Urine metabolites were less affected (only 3 metabolites significant at  $q$ -value) (Table S6C, Fig. S6). PCA on urine metabolites did not reveal a clear clustering on the different time points (PERMANOVA  $ns$ ) (Fig. S7A). Differently from the 2 other compartments, C-means clustering revealed an optimum of 9 clusters (Fig. S7C). Clusters 2, 3, 5, 6, 7 and 9 were more similar to each other than clusters 1, 4 and 8 according to the PCA on the centers of the clusters (Fig. S7B). The 3 significantly changed metabolites, acetate, hippurate and trimethylamine, were respectively members of cluster 1, 6 and 8 and were all significantly reduced at T4 (Fig. S7C, Fig. S6).

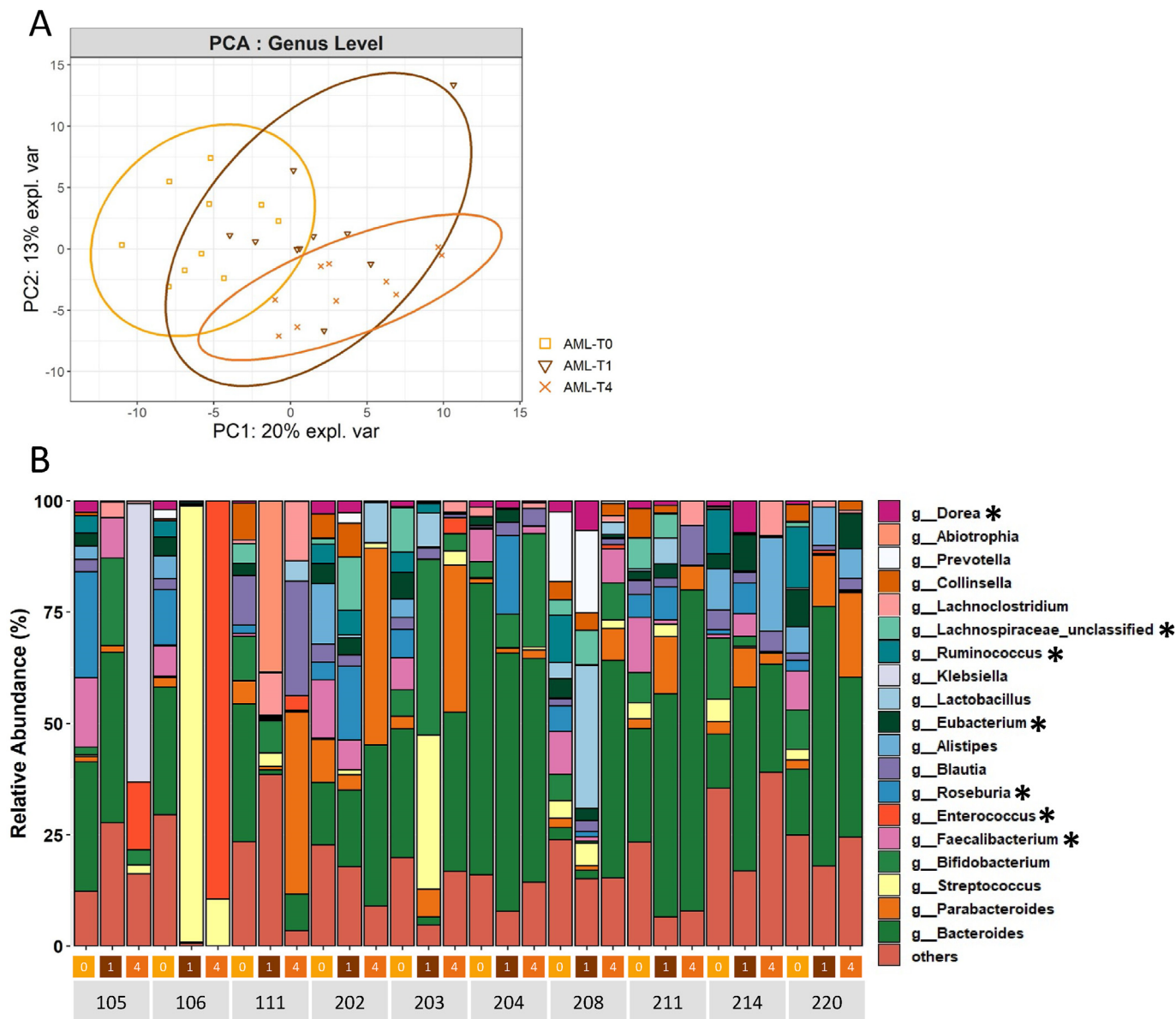


**Fig. 4.** Gut microbiota (genus level) evolution through inpatient stay. A) Principal component analysis (PCA) on all genera. PERMANOVA on the groups: R2: 17.8% (p-value = 0.001). B) Barplot with the 19 most abundant genera. Genera were tested with Friedman tests. \*: q-value < 0.05.

### 3.3. Specific bacterial changes occurring along AML intensive therapy associate to phenotypic alterations

To get an overview of the links and associations that could occur among the different datasets, we integrated the metabolomic and phenotypic data with the gut microbiota data (species, genera and diversity indices). As we aimed to gain insight from intra-individual patterns of change over time and distinguish them from inter-individual variations, we calculated the within-variance matrices and used these matrices for the integration using DIABLO [37]. Such analysis, when visualized as a circoplot, brought to light a deep interconnection between the 6 datasets with both positive and negative associations between the different datasets significant at high cut-offs (*r* cut-off of 0.8 in Fig. 8, *r* cut-off of 0.7 in Fig. S8) demonstrating the power of our experimental and statistical design. The model generated by DIABLO was also explored through a clustered image map (CIM) which is often used to explore high-dimensional datasets. The CIM revealed a clear clustering by

timing (Fig. 9). T1 was particularly separated from T0 and T4. There were also 3 clusters of variables. The top cluster grouped variables being reduced at T1 in comparison to T0 with *Clostridium disporicum*, *O. splanchnicus* (and parent genus), *Intestinibacter bartlettii* (and parent genus), citrulline, urine hippurate and Shannon index. The center cluster grouped variables that were mainly reduced at T4 in comparison to T0 and T1 with *Gemmiger formicillis*, the BMI, blood urea and urine urea. The bottom cluster concentrated variables that were mostly increased at T1 and T4 in comparison to T0 such as *C. concisus* (and parent genus), *Lactobacillus* and *E. faecium* (and parent genus), CRP and IL8.

### 4. Discussion

In this study, we investigated the changes in the gut microbiome induced by AML intense therapy and their association with gut barrier function and cachectic hallmarks. We found deep alterations in the gut microbiota composition and function, together

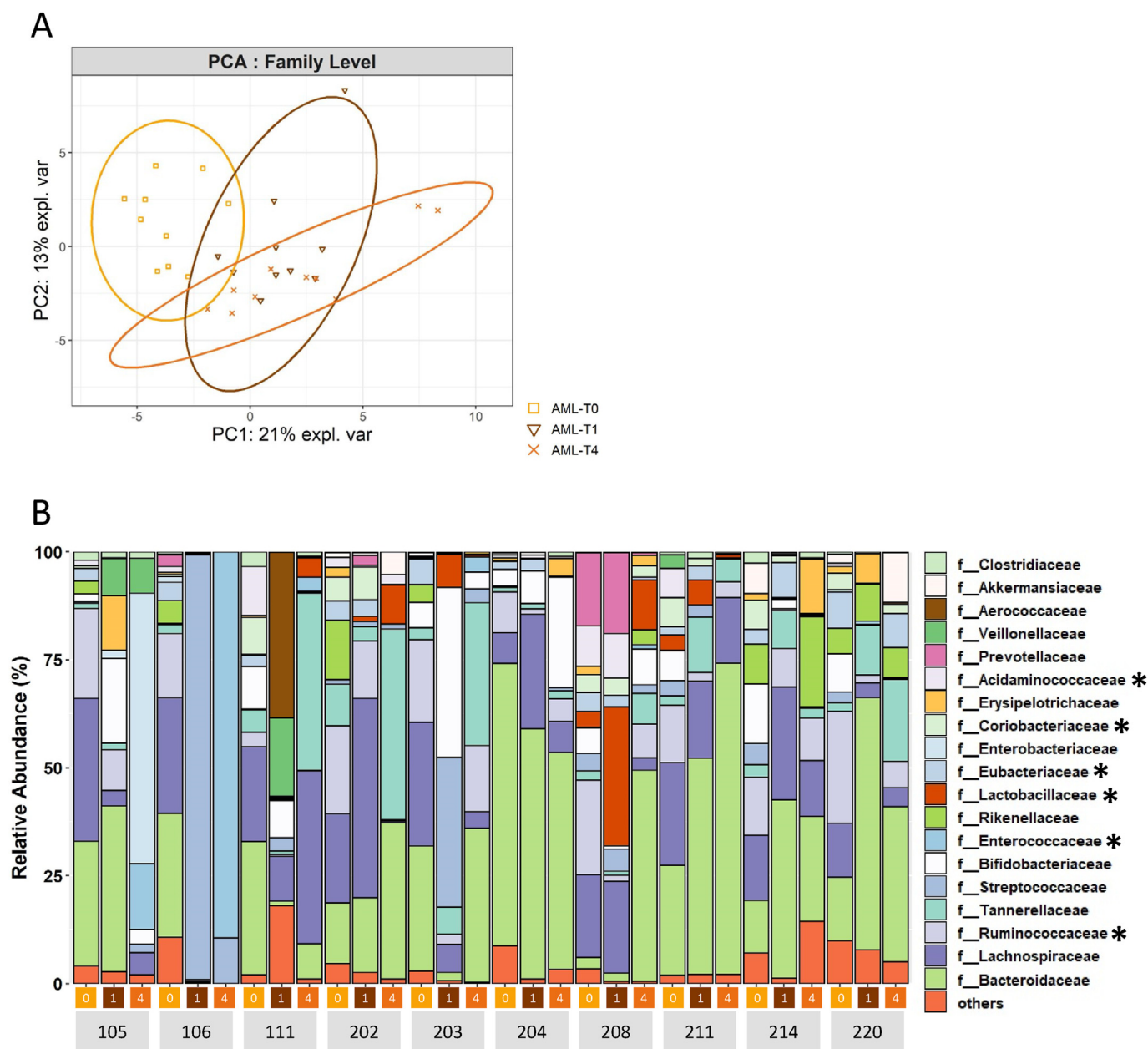


Fig. 5. Gut microbiota (family level) evolution through inpatient stay. A) Principal component analysis (PCA) on all genera. PERMANOVA on the groups: R2: 19.5% (p-value = 0.001). B) Barplot with the 19 most abundant families. Families were tested with Friedman tests. \*: q-value < 0.05.

with gut barrier dysfunction, high levels of systemic inflammation, muscle mass wasting, anorexia, and body weight loss after SIC (Fig. 10). The incidence of cachexia (50%) was in accordance with previous studies in the field [23].

We noticed major alterations of gut microbiota composition during the inpatient stay coherent with previous reports [4–6]. Despite the broad use of antibiotics, there was no change in total bacterial load in contrast to Hueso and colleagues' report [14]. Yet, the reduction in  $\alpha$ -diversity indexes and the differential abundance analyses concurred to indicate a lasting loss of numerous bacterial members at the benefit of a few others. This lack of change in bacterial load can be explained by the spectrum of the different antibiotics administered to the patients and the absence of combinations of antibiotics. In this study, by design, the effects of the chemotherapy were not differentiable from the ones of the

antibiotics. Interestingly, daunorubicin has been shown to hamper the growth of *O. splanchnicus* and several members of the *Clostridium* genus [45], which were significantly decreased at T1 and T4 in our cohort, while members of the *Lactobacillus* and *Enterococcus* genera, which have been shown to be insensitive to daunorubicin *in vitro* [46], were increased in our cohort.

*C. concisus*, an oral bacterium and opportunistic pathogen [47], was detected in 6 out of 10 patients after SIC (T1) in our cohort. Increased translocation of oral bacteria to the gut has been reported in many other pathological contexts, including AML, inflammatory bowel disease and liver cirrhosis (Pötgens et al., under consideration) [48,49], and has been shown to promote intestinal inflammation [48]. Interestingly, *C. concisus* is associated in the CIM to inflammatory markers such as serum CRP and IL8. A causal link for such association is supported by the observation that multiple

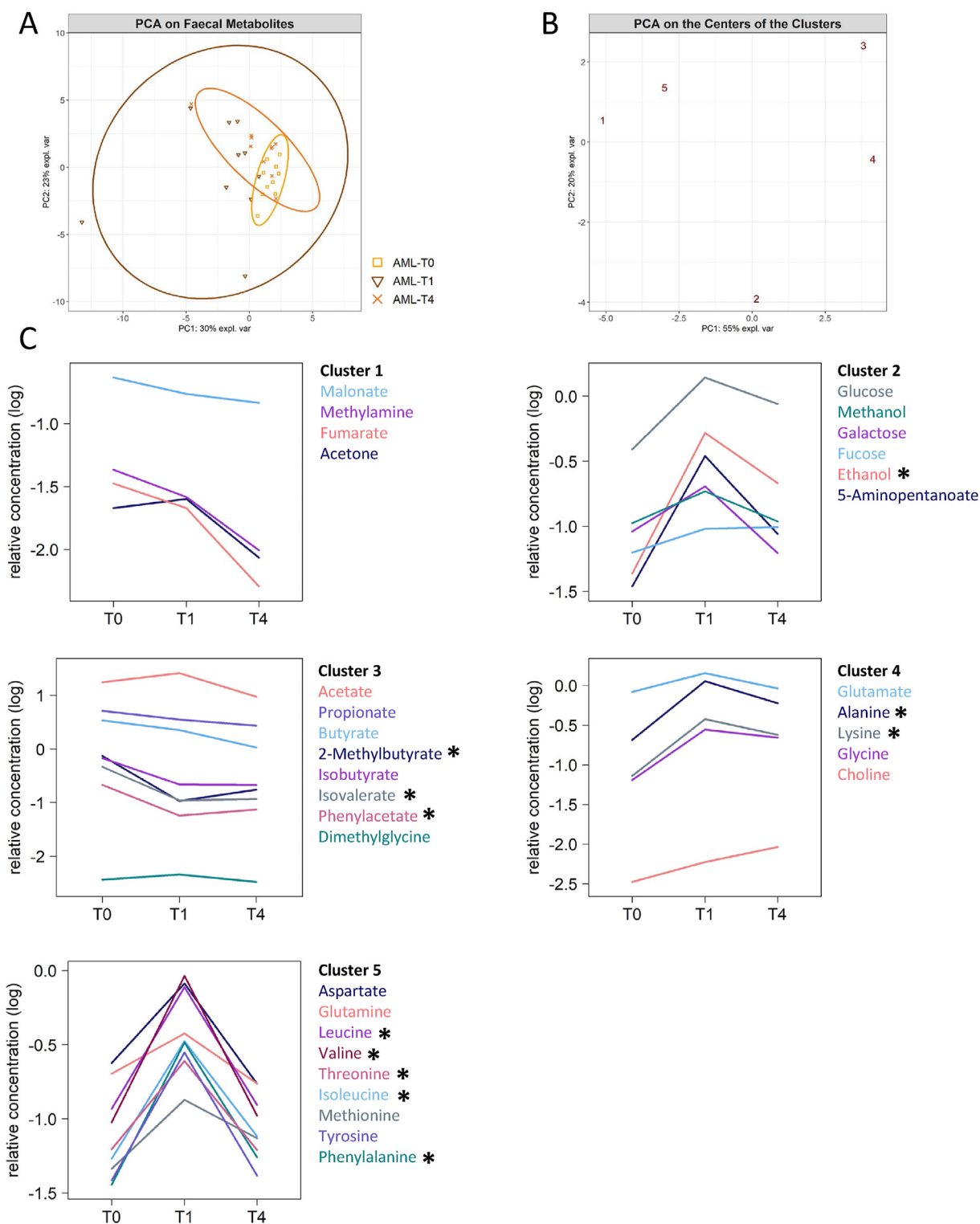


**Fig. 6.** Faecal metabolomics evolution through inpatient stay. A) Principal component analysis (PCA) on all faecal metabolites. PERMANOVA on the groups: R2: 16.4% (p-value = 0.01). B) PCA on the centers of the clusters of metabolites generated through C-means clustering (Mfuzz). C) Medians for the metabolites of all clusters. Friedman test\*: q-value < 0.05.

strains of *C. concisus* have been shown to induce the production of IL8 in intestinal cells *in vitro* [50].

*Lactobacillus* and *Enterococcus*, especially *E. faecium*, were also increased following SIC and selected by the integrative approach. The increase in *E. faecium* is coherent with its antibiotic's resistance

capacity [51] and previous reports [5,7]. *Lactobacillus* increase is less consistent: it did not occur in all patients of our cohort and was also not reported in all previous studies in AML patients [4,14,52]. The occurrence of *Lactobacillus* is unlikely to confer a protective effect on the gut barrier function since we noticed no correlation

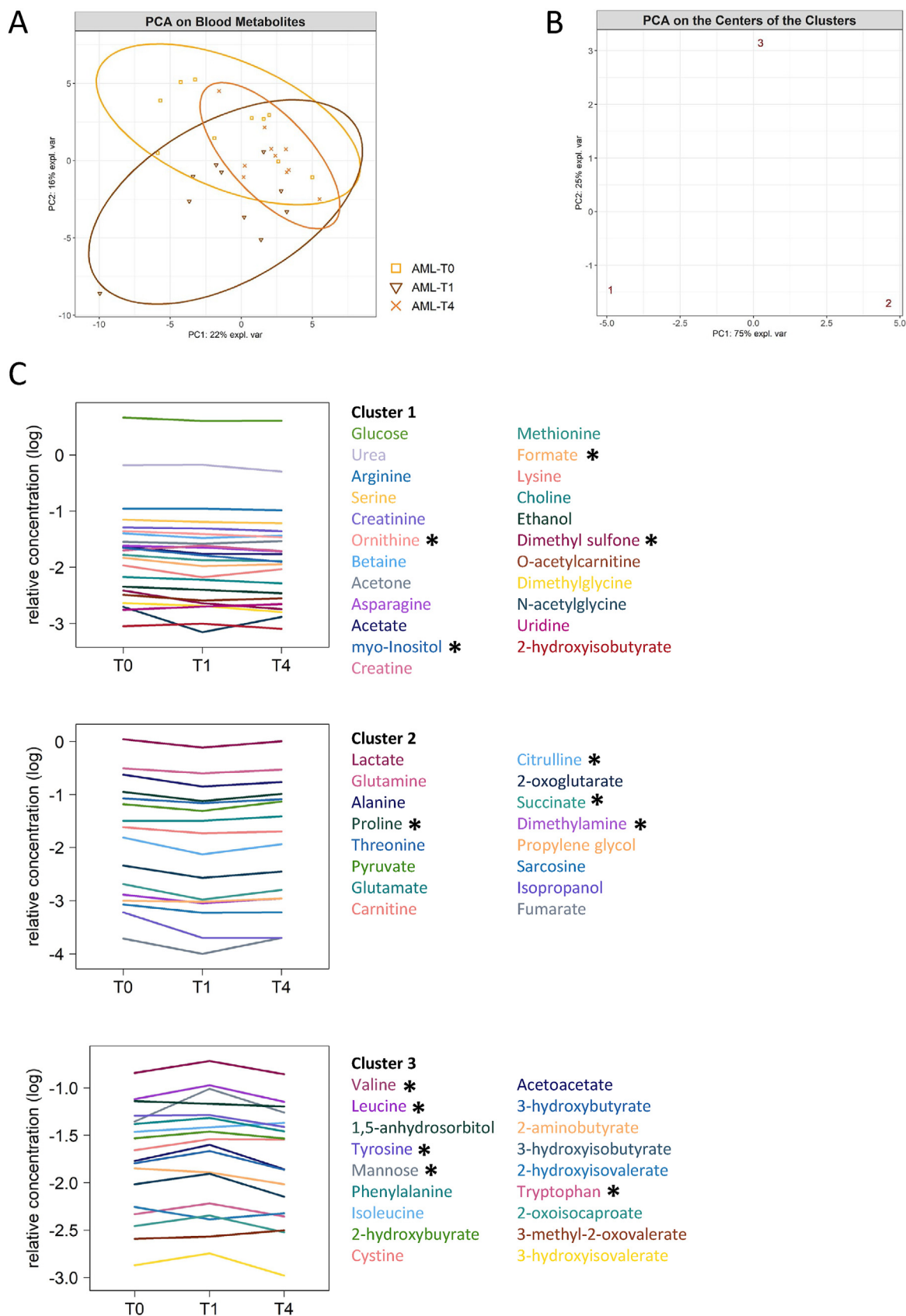


**Fig. 7.** Blood metabolomics evolution through inpatient stay. A) Principal component analysis (PCA) on all blood metabolites. PERMANOVA on the groups: R2: 10.5% (p-value = 0.02). B) PCA on the centers of the clusters of metabolites generated through C-means clustering (Mfuzz). C) Medians for the metabolites of all clusters. Friedman test \*: q-value < 0.05.

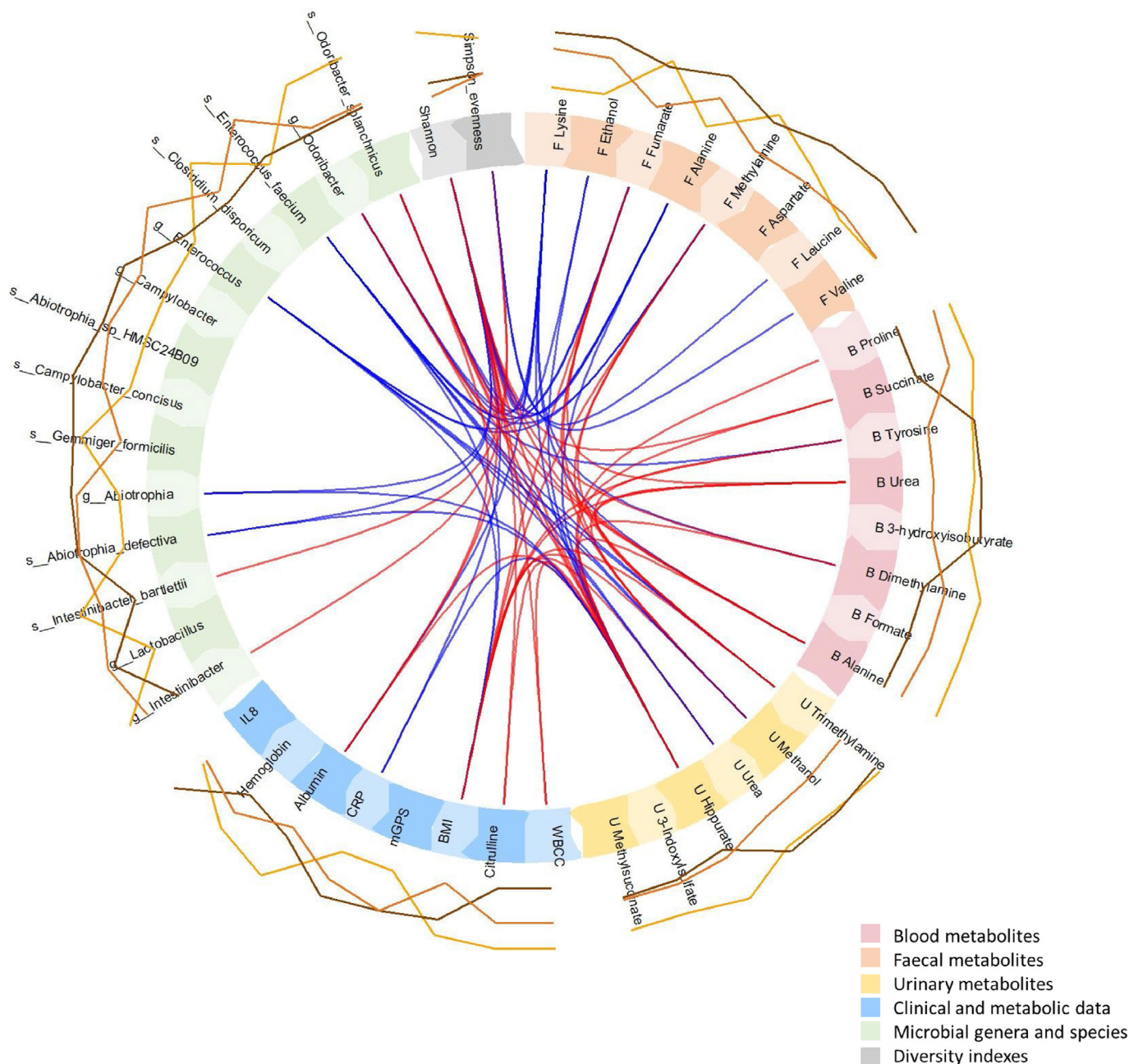


**Fig. 8.** Linked variables between metabolites, genera and species, diversity indexes and clinical, metabolic and inflammatory markers. Circoplot with a  $r$  cutoff = 0.8. Positive associations are in red and negative ones in blue. (For interpretation of the references to colour in this figure legend, the reader is referred to the Web version of this article.)

between *Lactobacillus* levels and gut barrier markers. The increase in *Lactobacillus* observed under AML treatment could be the result of its facultative anaerobe capacity and its ability to benefit from an increase in oxygen in the gut [53], similar to what has been previously reported for *Enterobacteriaceae* [54].

*I. bartlettii*, *O. splanchnicus* and *G. formicilis*, three short-chain fatty acid (SCFA) producers [55–58] were reduced after SIC. Despite those changes, we did not observe a reduction in faecal SCFA. However, faecal SCFA levels might not truly reflect SCFA production considering the absorption and utilization of SCFA by intestinal epithelial cells [59]. *I. bartlettii* is known for its association with metformin intake [60,61]. However, such explanation can be dismissed as there was no change in such drug intake during the inpatient stay. *G. formicilis* and *O. splanchnicus* have been previously

associated to a protective effect against pathogen infections such as *Clostridium difficile* [62,63]. Their decrease is thus coherent with the higher risk of hospitalized AML patient to develop an infection after SIC. Noteworthy, *G. formicilis* is the only bacterium present in the center cluster, which also includes the BMI, blood urea and urine urea. The BMI is a key indicator of cachexia while we evidenced reduction of urea as a sign of an altered AA metabolism in a pre-clinical model of cancer cachexia [33]. *G. formicilis* is a poorly explored bacterium; whether *G. formicilis* can affect host metabolism and energy homeostasis, particularly in the context of cancer cachexia, has never been investigated.

In a parallel study, we found a reduction of the gut barrier function in AML patients at diagnosis compared to healthy matched counterparts (Pötgens et al., under consideration). Here, we report

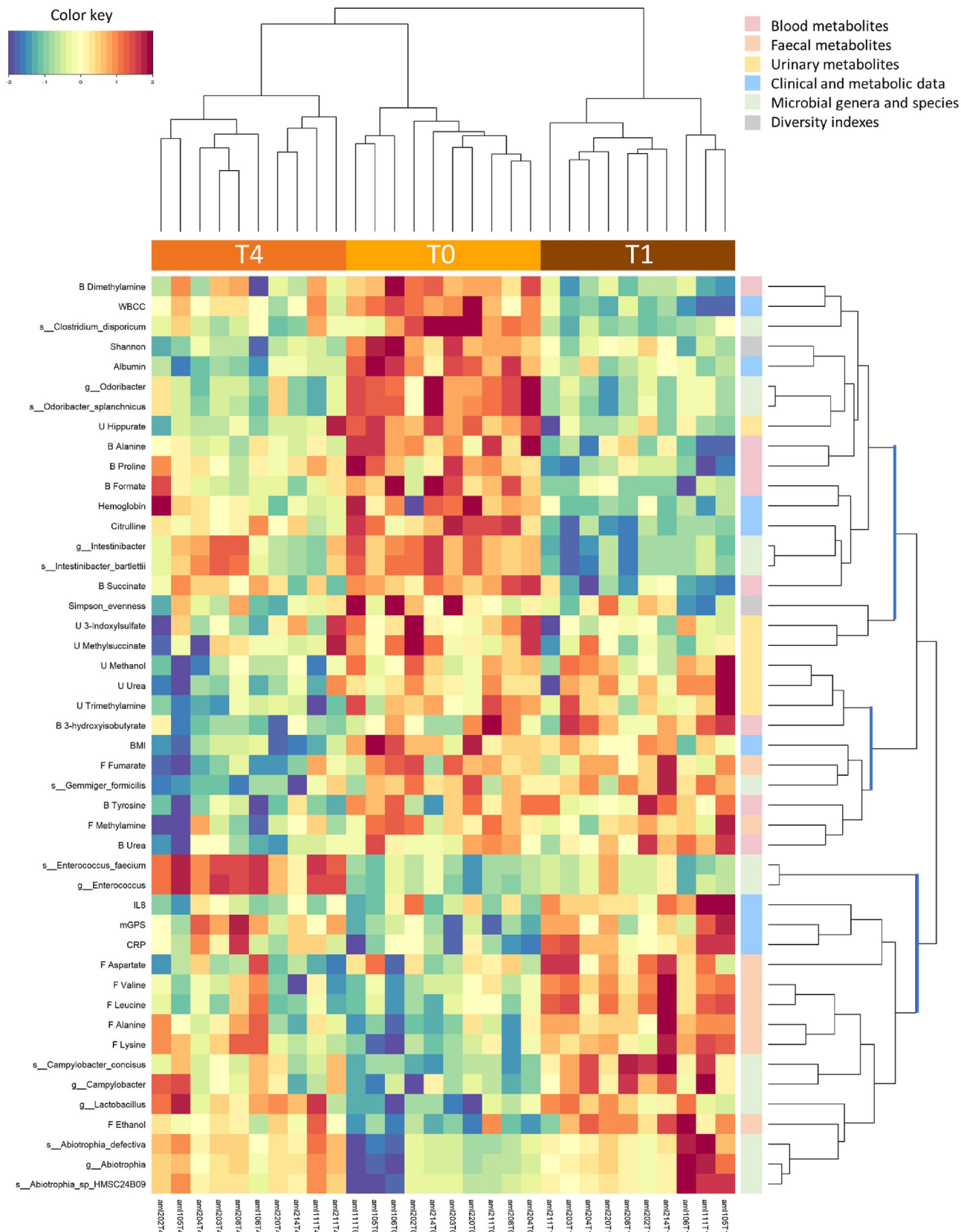


**Fig. 9.** Linked variables between metabolites, genera and species, diversity indexes and clinical, metabolic and inflammatory markers. Clustered image map (CIM) with dendrograms indicating the similarity level among samples and selected variables. Blue lines in the variable dendrogram indicate the 3 clusters of variables described in the text of the manuscript. Dataset origin is indicated by the color on the right side of the CIM. (For interpretation of the references to colour in this figure legend, the reader is referred to the Web version of this article.)

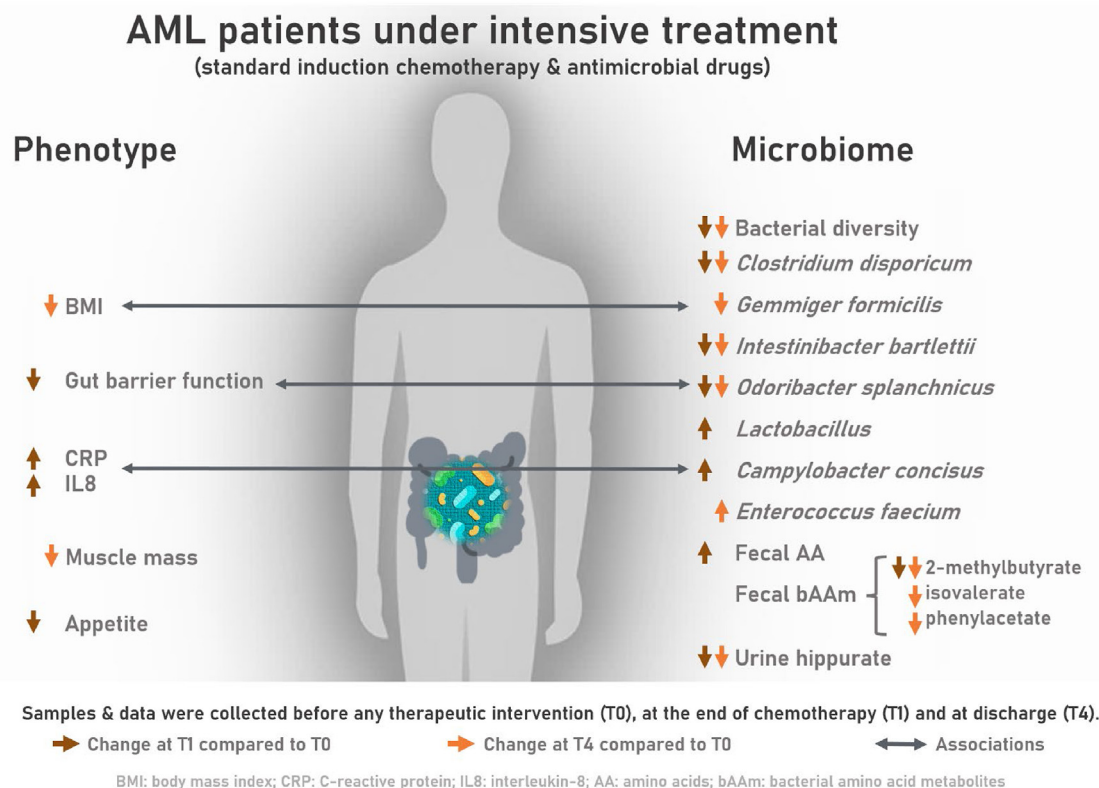


**Fig. 10.** Graphical abstract summarizing the most salient findings of the study “Gut microbiota alterations induced by intensive chemotherapy in acute myeloid leukaemia patients are associated with gut barrier dysfunction and body weight loss”.

that the AML intensive therapy further aggravates this parameter. The gut microbiome and the gut barrier function maintain a close relationship in which the alterations of one can drive a perturbation of the other. Among the bacteria associated to citrulline, the only one which was correlated to its reduction, reflecting gut barrier damage, was *O. splanchnicus* (Fig. S9). Patients with higher levels of *O. splanchnicus* at admission (T0) experienced a less intense gut barrier damage. Interestingly, the administration of this species was sufficient to confer resistance against colitis and colorectal cancer in mice [64], supporting our hypothesis that this bacterium may also play a protective effect in AML patients.

One of the main changes observed in the metabolomics results is the important increase of AA in faeces at T1 and a reduction in bAAm. Interestingly, AA levels were reduced at T4 while bAAm levels were not restored. This suggests that although some metabolites returned to their initial levels, the gut microbial activity linked to those metabolites did not. A second example of such reduced bacterial activity comes from the levels of urine hippurate, which are reduced by 4-fold both at T1 and T4. Those data demonstrate the long-lasting shift in the gut microbiota activity due to SIC and associated treatments, complementing previous reports highlighting an altered bacterial composition.

The originality of our study lies in the use of several *-omics* analyses on the same patients at defined time points and the exploitation of integrative approaches, to an extent not achieved so far. Another strength of our design is the use of those data to gain insight into common intra-individual patterns of change over time and distinguish them from inter-individual variations attributed among others to the unique features of one's gut microbiota. Our study also presents several limitations. We used strict inclusion and exclusion criteria to avoid the classical bias in the field of gut microbiota studies and to ensure a uniform cohort, but this

inherently limited the number of patients included in the study and might limit the generalization of the results. However, despite the small size of this exploratory cohort, we were able to see major and significant changes linked to AML intensive treatment that were concordant with a comparable study [14], suggesting that the power of our study to detect key microbial changes and metabolic and inflammatory alterations was sufficient. The high number of associations detected at a high cut-off level using DIABLO was also indicative of a sufficient statistical power to address our exploratory objective. Those aspects reinforce the relevance of our study and suggest the need for larger clinical studies in the field.

In conclusion, our study reveals that AML intensive therapy transiently impairs the gut barrier function while inducing enduring alterations in the composition and metabolic activity of the gut microbiota. Such alterations are associated with cachectic hallmarks such as body weight loss and inflammation. Importantly, we identified bacteria whose disappearance was associated with impaired gut barrier function (*O. splanchnicus*) and body weight loss (*G. formicilis*), suggesting that these bacteria may represent actionable targets to improve supportive care in AML patients. These findings will be essential to guide clinically relevant future mechanistic research aiming at eventually complementing AML intensive treatment with microbiota-based therapeutic strategies. Furthermore, microbiota profiling strategies based on these species might also be helpful for risk stratification towards cachexia and gut barrier dysfunction.

### Funding

This work was funded by an ESPEN Research fellowship awarded to LBB, the Fonds de la Recherche Scientifique – FNRS (F.R.S.-FNRS) under Grant MIS F.4512.20 and the Fonds Wetenschappelijk

Onderzoek – Vlaanderen (FWO) and the F.R.S. – FNRS under EOS Project No. 40007505. This work would not have been possible without the support of the Télévie (Intercachectomics consortium) and the Louvain Foundation. LBB is also the recipient of subsidies from the FSR (Fonds Spéciaux de la Recherche, UCLouvain, including the Action de Recherche Concertée LIPOCAN (19–24.096)) and from the Walloon Region in the context of the funding of the strategic axis FRFS-WELBIO (40009849). LBB is a Collen-Francqui Research Professor and grateful for the support of the Francqui Foundation. The funders had no role in study design, data collection and analysis, interpretation of the results, decision to publish or preparation of the manuscript.

### Authors' contributions

Conception & design of the work: SAP, NMD, LBB. Contribution to the design of the clinical study and ensuing analyses: VH, HS. Clinical data collection and biological sampling: SAP, VH, JM, HS, LBB. Clinical data analyses: SAP. Metabolomics analysis: SAP, with the help of SL for urinary metabolomics. Microbiome analyses: SAP, FL, JW, LBB. Analyses of metabolic and inflammatory markers: SAP, ANM, LBB. Citrulline analysis by mass spectrometry: NN. Data integration: SAP. Data interpretation: SAP, LBB. Contribution to data interpretation: VH, HS, JW, NMD. Acquisition of funding: LBB. Supervision of the work: LBB. Drafting the article: SAP, LBB. Revision of the article: all. Final approval of the version to be published: all.

### Availability of data and materials

Full details on the methods described in this paper are provided in the Supporting Information. Raw sequences on 16S rRNA gene sequencing and shotgun sequencing can be found in the SRA database (projects ID: PRJNA813705 (T0) and PRJNA875377 (T1–T4)).

### Conflicts of interest

HS reports having received personal fees from Incyte, Janssen, Novartis, Sanofi and from the Belgian Hematological Society (BHS), as well as research grants from Novartis and the BHS, all paid to her institution. She has also received non-financial support (travel grants) from Gilead, Pfizer, the EBMT (European Society for Blood and Marrow transplantation) and the CIBMTR (Center for International Bone Marrow Transplantation Research). None of these potential conflicts of interest are relevant to this project. All other authors declare no conflict of interest.

### Acknowledgments

The authors gratefully thank all the study participants. The authors are grateful to Myriam Cleeren, Jill Pannecoucke, Vera Ciku and Isabelle Blave, as well as the data nurses and the medical team involved in the study, for their help in the collection of the biological samples and clinical data. SAP and LBB thank Prof Jean-Baptiste Demoulin for his advice during the study design, Martin Nicolas and Bouazza Es Saadi for providing technical assistance during sample analyses, Dr Nicolas Joudiou and the UCLouvain-LDRI Nuclear and Electron Spin Technologies (NEST) platform for providing easy access and skilled assistance to the NMR spectrometer, Prof Ana Beloqui for access to a Meso Scale Discovery microplate reader, and Dr Céline Bugli and the Statistical Methodology and Computing Service, a technological platform at UCLouvain – SMCS/LIDAM, UCLouvain for their advice. The authors also acknowledge the Centre d'expertise et de services Génome Québec (shotgun sequencing) and the University of Minnesota Genomics

Centre for (16S rRNA gene sequencing) for their sequencing services and support.

### Appendix A. Supplementary data

Supplementary data to this article can be found online at <https://doi.org/10.1016/j.clnu.2023.09.021>.

### References

- [1] Short NJ, Rytting ME, Cortes JE. Acute myeloid leukaemia. *Lancet* 2018;392(10147):593–606.
- [2] Lee JH, Kim H, Joo YD, Lee WS, Bae SH, Zang DY, et al. Prospective randomized comparison of idarubicin and high-dose daunorubicin in induction chemotherapy for newly diagnosed acute myeloid leukemia. *J Clin Oncol* 2017;35(24):2754–63.
- [3] Adige S, Lapidus RG, Carter-Cooper BA, Duffy A, Patzke C, Law JY, et al. Equipotent doses of daunorubicin and idarubicin for AML: a meta-analysis of clinical trials versus in vitro estimation. *Cancer Chemother Pharmacol* 2019;83(6):1105–12.
- [4] Galloway-Pena JR, Smith DP, Sahasrabhojane P, Ajami NJ, Wadsworth WD, Daver NG, et al. The role of the gastrointestinal microbiome in infectious complications during induction chemotherapy for acute myeloid leukemia. *Cancer* 2016;122(14):2186–96.
- [5] Rashidi A, Kaiser T, Shields-Cutler R, Graiziger C, Holtan SG, Rehman TU, et al. Dysbiosis patterns during re-induction/salvage versus induction chemotherapy for acute leukemia. *Sci Rep* 2019;9(1):6083.
- [6] Rashidi A, Kaiser T, Graiziger C, Holtan SG, Rehman TU, Weisdorf DJ, et al. Gut dysbiosis during antileukemia chemotherapy versus allogeneic hematopoietic cell transplantation. *Cancer* 2020;126(7):1434–47.
- [7] Rashidi A, Ebadi M, Rehman TU, Elhousseini H, Nalluri H, Kaiser T, et al. Altered microbiota-host metabolic cross talk preceding neutropenic fever in patients with acute leukemia. *Blood Adv* 2021;5(20):3937–50.
- [8] Rashidi A, Kaiser T, Graiziger C, Holtan SG, Rehman TU, Weisdorf DJ, et al. Specific gut microbiota changes heralding bloodstream infection and neutropenic fever during intensive chemotherapy. *Leukemia* 2020;34(1):312–6.
- [9] Rattanathammethee T, Tuitemwong P, Thiennimitr P, Sarichai P, Pombeyra SN, Piriyaakuntorn P, et al. Gut microbiota profiles of treatment-naïve adult acute myeloid leukemia patients with neutropenic fever during intensive chemotherapy. *PLoS One* 2020;15(10):e0236460.
- [10] Taur Y, Jenq RR, Perales MA, Littmann ER, Morjaria S, Ling L, et al. The effects of intestinal tract bacterial diversity on mortality following allogeneic hematopoietic stem cell transplantation. *Blood* 2014;124(7):1174–82.
- [11] Jenq RR, Taur Y, Devlin SM, Ponce DM, Goldberg JD, Ahr KF, et al. Intestinal blautia is associated with reduced death from graft-versus-host disease. *Biol Blood Marrow Transplant* 2015;21(8):1373–83.
- [12] Peled JU, Gomes ALC, Devlin SM, Littmann ER, Taur Y, Sung AD, et al. Microbiota as predictor of mortality in allogeneic hematopoietic-cell transplantation. *N Engl J Med* 2020;382(9):822–34.
- [13] Bow EJ, Loewen R, Cheang MS, Shore TB, Rubinger M, Schacter B. Cytotoxic therapy-induced D-xylose malabsorption and invasive infection during remission-induction therapy for acute myeloid leukemia in adults. *J Clin Oncol* 1997;15(6):2254–61.
- [14] Hueso T, Ekpe K, Mayeur C, Gatsé A, Curt MJC, Gricourt G, et al. Impact and consequences of intensive chemotherapy on intestinal barrier and microbiota in acute myeloid leukemia: the role of mucosal strengthening. *Gut Microb* 2020;12(1):1800897.
- [15] D'Angelo CR, Sudakaran S, Callander NS. Clinical effects and applications of the gut microbiome in hematologic malignancies. *Cancer* 2021;127(5):679–87.
- [16] Caballero-Flores G, Pickard JM, Nunez G. Microbiota-mediated colonization resistance: mechanisms and regulation. *Nat Rev Microbiol* 2023;21(6):347–60.
- [17] Yu LC, Shih YA, Wu LL, Lin YD, Kuo WT, Peng WH, et al. Enteric dysbiosis promotes antibiotic-resistant bacterial infection: systemic dissemination of resistant and commensal bacteria through epithelial transcytosis. *Am J Physiol Gastrointest Liver Physiol* 2014;307(8):G824–35.
- [18] Rashidi A, Ebadi M, Rehman TU, Elhousseini H, Halaweish HF, Kaiser T, et al. Lasting shift in the gut microbiota in patients with acute myeloid leukemia. *Blood Adv* 2022;6(11):3451–7.
- [19] Nakamura N, Ninomiya S, Matsumoto T, Nakamura H, Kitagawa J, Shiraki M, et al. Prognostic impact of skeletal muscle assessed by computed tomography in patients with acute myeloid leukemia. *Ann Hematol* 2019;98(2):351–9.
- [20] Jung J, Lee E, Shim H, Park JH, Eom HS, Lee H. Prediction of clinical outcomes through assessment of sarcopenia and adipopenia using computed tomography in adult patients with acute myeloid leukemia. *Int J Hematol* 2021;114(1):44–52.
- [21] Ando T, Fujisawa S, Teshigawara H, Ogusa E, Ishii Y, Miyashita K, et al. Impact of treatment-related weight changes from diagnosis to hematopoietic stem-cell transplantation on clinical outcome of acute myeloid leukemia. *Int J Hematol* 2019;109(6):673–83.
- [22] Paval DR, Patton R, McDonald J, Skipworth RJE, Gallagher IJ, Laird BJ. A systematic review examining the relationship between cytokines and

- cachexia in incurable cancer. *J Cachexia Sarcopenia Muscle* 2022;13(2): 824–38.
- [23] Pressoir M, Desne S, Berchery D, Rossignol G, Poiree B, Meslier M, et al. Prevalence, risk factors and clinical implications of malnutrition in French Comprehensive Cancer Centres. *Br J Cancer* 2010;102(6):966–71.
- [24] Campelj DG, Timpani CA, Rybalka E. Cachectic muscle wasting in acute myeloid leukaemia: a sleeping giant with dire clinical consequences. *J Cachexia Sarcopenia Muscle* 2022;13(1):42–54.
- [25] Bindels LB, Beck R, Schakman O, Martin JC, De Backer F, Sohet FM, et al. Restoring specific lactobacilli levels decreases inflammation and muscle atrophy markers in an acute leukemia mouse model. *PLoS One* 2012;7(6): e37971.
- [26] Bindels LB, Neyrinck AM, Salazar N, Taminiau B, Druart C, Muccioli GG, et al. Non digestible oligosaccharides modulate the gut microbiota to control the development of leukemia and associated cachexia in mice. *PLoS One* 2015;10(6):e0131009.
- [27] Bindels LB, Neyrinck AM, Claus SP, Le Roy CI, Granette C, Pot B, et al. Synbiotic approach restores intestinal homeostasis and prolongs survival in leukaemic mice with cachexia. *ISME J* 2016;10(6):1456–70.
- [28] Rashidi A, Ebadi M, Rehman TU, Elhuisseini H, Halaweish H, Kaiser T, et al. Compilation of longitudinal gut microbiome, serum metabolome, and clinical data in acute myeloid leukemia. *Sci Data* 2022;9(1):468.
- [29] Kim D, Hofstaedter CE, Zhao C, Mattei L, Tanes C, Clarke E, et al. Optimizing methods and dodging pitfalls in microbiome research. *Microbiome* 2017;5(1): 52.
- [30] Wilson MM, Thomas DR, Rubenstein LZ, Chibnall JT, Anderson S, Baxi A, et al. Appetite assessment: simple appetite questionnaire predicts weight loss in community-dwelling adults and nursing home residents. *Am J Clin Nutr* 2005;82(5):1074–81.
- [31] Neveux N, David P, Cynober L. Measurement of amino acid concentration in biological fluids and tissues using ion-exchange chromatography. In: CL, editor. *Metabolic and therapeutic aspects of amino acids in clinical nutrition*. 2nd ed. Boca Raton, FL: CRC Press; 2004. p. 17–28.
- [32] Costea PI, Zeller G, Sunagawa S, Pelletier E, Alberti A, Levenez F, et al. Towards standards for human fecal sample processing in metagenomic studies. *Nat Biotechnol* 2017;35(11):1069–76.
- [33] Pötgens SA, Thibaut MM, Joudiou N, Sboarina M, Neyrinck AM, Cani PD, et al. Multi-compartment metabolomics and metagenomics reveal major hepatic and intestinal disturbances in cancer cachectic mice. *J Cachexia Sarcopenia Muscle* 2021;12(2):456–75.
- [34] Wishart DS, Feunang YD, Marcu A, Guo AC, Liang K, Vázquez-Fresno R, et al. HMDB 4.0: the human metabolome database for 2018. *Nucleic Acids Res* 2018;46(D1):D608–17.
- [35] Benjamini Y, Hochberg Y. Controlling the false discovery rate: a practical and powerful approach to multiple testing. *J Roy Stat Soc B* 1995;57(1): 289–300.
- [36] Kumar L, M E. Mfuzz: a software package for soft clustering of microarray data. *Bioinformatics* 2007;21(1):5–7.
- [37] Singh A, Shannon CP, Gautier B, Rohart F, Vacher M, Tebbutt SJ, et al. DIABLO: an integrative approach for identifying key molecular drivers from multi-omics assays. *Bioinformatics* 2019;35(17):3055–62.
- [38] Rohart F, Gautier B, Singh A, Lê Cao KA. mixOmics: an R package for 'omics feature selection and multiple data integration. *PLoS Comput Biol* 2017;13(11).
- [39] Fearon K, Strasser F, Anker SD, Bosaeus I, Bruera E, Fainsinger RL, et al. Definition and classification of cancer cachexia: an international consensus. *Lancet Oncol* 2011;12(5):489–95.
- [40] Breen DM, Kim H, Bennett D, Calle RA, Collins S, Esquejo RM, et al. GDF-15 neutralization alleviates platinum-based chemotherapy-induced emesis, anorexia, and weight loss in mice and nonhuman primates. *Cell Metabol* 2020;32(6):938–950 e6.
- [41] Liu H, Zhai Y, Zhao W, Wan Y, Lu W, Yang S, et al. Consolidation chemotherapy prevents relapse by indirectly regulating bone marrow adipogenesis in patients with acute myeloid leukemia. *Cell Physiol Biochem* 2018;45(6): 2389–400.
- [42] Sartori R, Romanello V, Sandri M. Mechanisms of muscle atrophy and hypertrophy: implications in health and disease. *Nat Commun* 2021;12(1): 330.
- [43] Crenn P, Vahedi K, Lavergne-Slove A, Cynober L, Matuchansky C, Messing B. Plasma citrulline: a marker of enterocyte mass in villous atrophy-associated small bowel disease. *Gastroenterology* 2003;124(5):1210–9.
- [44] Lefevre C, Bindels LB. Role of the gut microbiome in skeletal muscle physiology and pathophysiology. *Curr Osteoporos Rep* 2022;20(6):422–32.
- [45] Maier L, Pruteanu M, Kuhn M, Zeller G, Telzerow A, Anderson EE, et al. Extensive impact of non-antibiotic drugs on human gut bacteria. *Nature* 2018;555(7698):623–8.
- [46] van Vliet MJ, Tissing WJ, Dun CA, Meessen NEL, Kamps WA, De Bont ESJM, et al. Chemotherapy treatment in pediatric patients with acute myeloid leukemia receiving antimicrobial prophylaxis leads to a relative increase of colonization with potentially pathogenic bacteria in the gut. *Clin Infect Dis* 2009;49(2):262–70.
- [47] Istivan TS, Smith SC, Fry BN, Coloe PJ. Characterization of *Campylobacter concisus* hemolysins. *FEMS Immunol Med Microbiol* 2008;54(2):224–35.
- [48] Atarashi K, Suda W, Luo C, Kawaguchi T, Motoo I, Narushima S, et al. Ectopic colonization of oral bacteria in the intestine drives TH1 cell induction and inflammation. *Science* 2017;358(6361):359–65.
- [49] Jin S, Wetzel D, Schirmer M. Deciphering mechanisms and implications of bacterial translocation in human health and disease. *Curr Opin Microbiol* 2022;67:102147.
- [50] Yde Aagaard ME, Frahm Kirk K, Linde Nielsen H, Steffensen R, Nielsen H. *Campylobacter concisus* from chronic inflammatory bowel diseases stimulates IL-8 production in HT-29 cells. *Gut Pathog* 2023;15(1):5.
- [51] Carvalho AS, Lagana D, Catford J, Shaw D, Bak N. Bloodstream infections in neutropenic patients with haematological malignancies. *Infect Dis Health* 2020;25(1):22–9.
- [52] Shen Z, Gu X, Cao H, Mao W, Yang L, He M, et al. Characterization of microbiota in acute leukemia patients following successful remission induction chemotherapy without antimicrobial prophylaxis. *Int Microbiol* 2021;24(2): 263–73.
- [53] Hartman AL, Lough DM, Barupal DK, Fiehn O, Fishbein T, Zasloff M, et al. Human gut microbiome adopts an alternative state following small bowel transplantation. *Proc Natl Acad Sci U S A* 2009;106(40):17187–92.
- [54] Rivera-Chavez F, Lopez CA, Baumler AJ. Oxygen as a driver of gut dysbiosis. *Free Radic Biol Med* 2017;105:93–101.
- [55] Song YL, Liu CX, McTeague M, Summanen P, Finegold SM. *Clostridium bartlettii* sp. nov., isolated from human faeces. *Anaerobe* 2004;10(3):179–84.
- [56] Nagai F, Morotomi M, Watanabe Y, Sakon H, Tanaka R. *Alistipes indistinctus* sp. nov. and *Odoribacter laneus* sp. nov., common members of the human intestinal microbiota isolated from faeces. *Int J Syst Evol Microbiol* 2010;60(Pt 6):1296–302.
- [57] Salanitro JP, Muirhead PA, Goodman JR. Morphological and physiological characteristics of *Gemmiger formicilis* isolated from chicken ceca. *Appl Environ Microbiol* 1976;32(4):623–32.
- [58] Hiippala K, Barreto G, Burrello C, Diaz-Basabe A, Suutarinen M, Kainulainen V, et al. Novel *odoribacter splanchnicus* strain and its outer membrane vesicles exert immunoregulatory effects in vitro. *Front Microbiol* 2020;11:575455.
- [59] Boets E, Deroover L, Houben E, Vermeulen K, Gomand SV, Delcour JA, et al. Quantification of in vivo colonic short chain fatty acid production from inulin. *Nutrients* 2015;7(11):8916–29.
- [60] Forslund K, Hildebrand F, Nielsen T, Falony G, Le Chatelier E, Sunagawa S, et al. Disentangling type 2 diabetes and metformin treatment signatures in the human gut microbiota. *Nature* 2015;528(7581):262–6.
- [61] Wu H, Esteve E, Tremaroli V, Khan MT, Caesar R, Mannerås-Holm L, et al. Metformin alters the gut microbiome of individuals with treatment-naïve type 2 diabetes, contributing to the therapeutic effects of the drug. *Nat Med* 2017;23(7):850–8.
- [62] Sato Y, Atarashi K, Plichta DR, Arai Y, Sasajima S, Kearney SM, et al. Novel bile acid biosynthetic pathways are enriched in the microbiome of centenarians. *Nature* 2021;599(7885):458–64.
- [63] Solbach P, Chhatwal P, Woltemate S, Tacconelli E, Buhl M, Autenrieth IB, et al. Microbiota-associated risk factors for *clostridioides difficile* acquisition in hospitalized patients: a prospective, multicentric study. *Clin Infect Dis* 2021;73(9):e2625–34.
- [64] Xing C, Wang M, Ajibade AA, Tan P, Fu C, Chen L, et al. Microbiota regulate innate immune signaling and protective immunity against cancer. *Cell Host Microbe* 2021;29(6):959–974.e7.